Final Project: Induction Heater
ECE-394 Junior Projects

Evan Murphy   Thomas Coor   Cat Van West

May '23

Abstract

A single-mug induction heater was designed, simulated, and constructed using common electronic components and DC power supplies. The heater creates an alternating magnetic field in the vicinity of the target mug, which is transformed into thermal energy by eddy currents in a high-permeability material placed inside the mug. The heater utilizes a dual-resonant load design, allowing for high currents to flow through the heating coil, with low power consumption during operation.

Contents

1 Introduction

Induction heating was first developed in the early 1900s using spark gap oscillators, and by 1922 dedicated motor generators made medium power heating possible. The development of power semiconductors in the 1960s, however, made induction heating a practical industrial technology [1]. Induction heating is now well-established, used for industrial fabrication, domestic cooking, etc. More modern resonant topologies, spurred by the development of efficient gate drive schemes, have attracted interest for their improved efficiency over hard-switched topologies [2], [3].

We chose to build an induction heater for our final project. Our circuit consisted roughly of the following parts:

- a variable-frequency square-wave oscillator, based on a 7555,

- a gate drive circuit, consisting of two LM311 comparators & two push-pull followers built with junction transistors,

- a full-bridge of FETs, switched using a gate drive transformer, and

- a series-parallel LC circuit as a load, one of the inductors being the work coil itself.
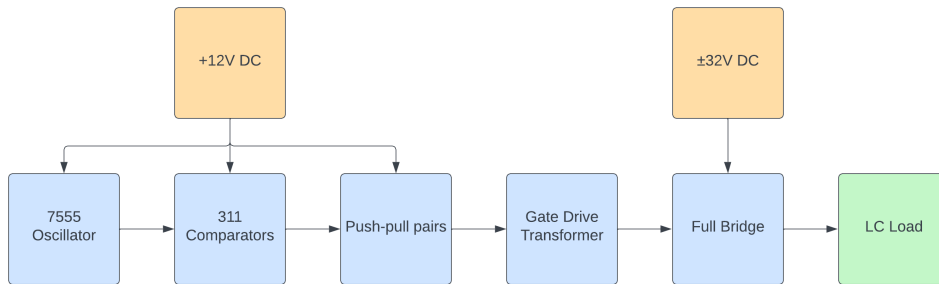
Figure 1: Block-diagram of the different sub-systems present in our heater design.

We used a dual LC coil for efficiency reasons: to effectively heat metal, large currents (many tens of amps) must flow through the work coil. Using the circuit we did reduce the current that must flow in the full-bridge for such operation.

The project turned out to be successful! The result of a late-stage test is given in figure 2.
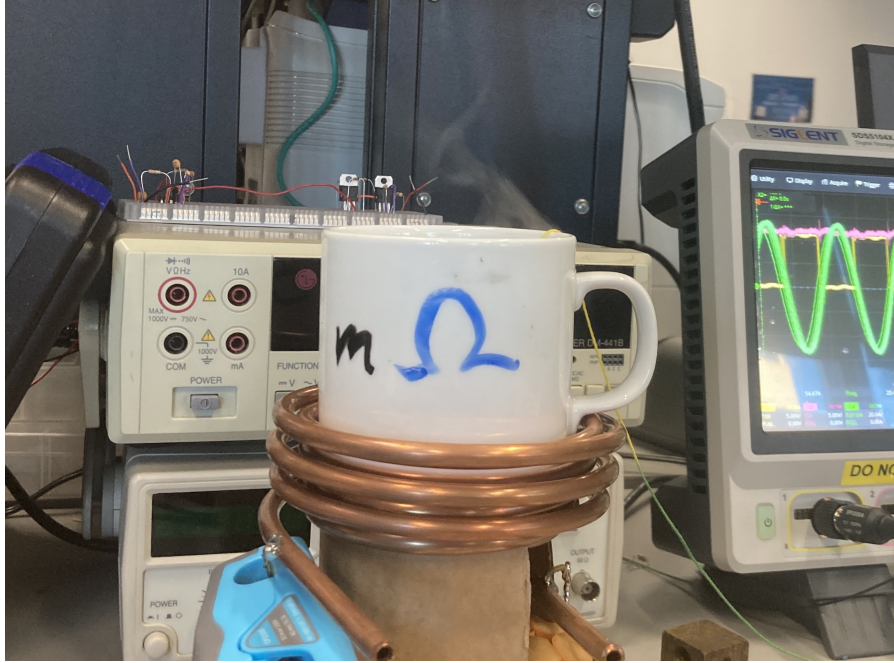

Figure 2: A mug of soon-to-be-tea, heated to around 70 °C.

2   Control Circuit Design

The design of the control circuitry was relatively straightforward. Most of it was derived directly or almost directly from prior work (i.e., the oscillator design used was one we had built earlier).

2.1   Oscillator

The core oscillator is based on a 7555 running in astable mode. Our circuit is given in figure 3.
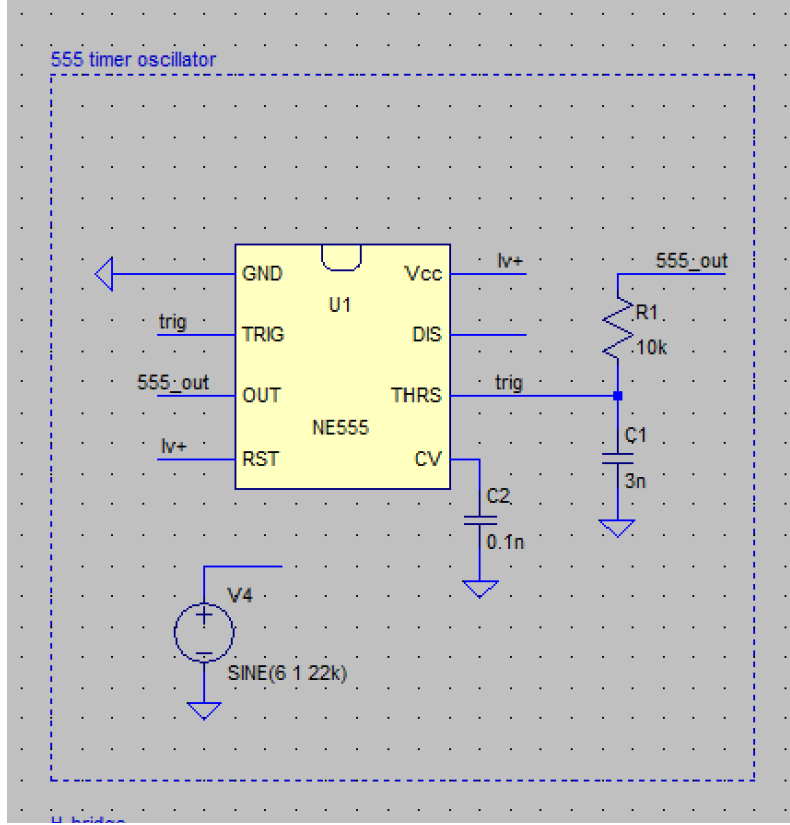
Figure 3: A 7555 timer-based oscillator with adjustable duty cycle.

We designed the oscillator to run at a fixed duty cycle of 50%, but with variable frequency to permit tuning for different loads (as we tested several).

2.2 Gate Signal Generation

The square wave signal exiting the 7555 had a slow slew rate relative to its period, though it was at the right frequency. We cleaned up the signal by using two daisy-chained LM311 comparators, as seen in figure 4. These snap between the two levels of the square wave. Using two in series generated two square waves 180° out of phase, which we fed into two push-pull followers to reduce their source impedance in preparation for driving the full bridge.
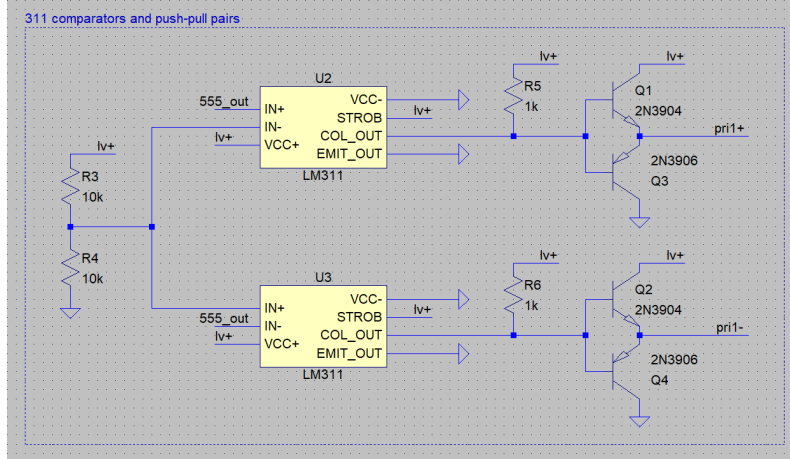
5

Figure 4: Two LM311s, along with followers.

2.3 Gate Drive Transformer

To drive a full bridge of 4 transistors using effectively a single drive signal, we employed a gate drive transformer (or GDT). A GDT is used to apply a drive signal directly between the gate and source (or base and emitter) of a switching transistor for whom, notably, the source is not necessarily ground-referenced. A small example (to be discussed) is given in figure 19, and the circuit we used is given in figure 5 in the next section.

The concept illustrated in figure 19 is as follows: Q1's emitter is not at ground, but sitting at the negative rail. In order to switch it on conventionally, a proper voltage above the negative rail would have to be applied to its base, which can be very difficult with low-voltage drive circuit components – especially if the negative rail is several hundred volts below ground! Thus, Q1 is driven through a transformer. This has two benefits: one, Q1's base is always at the correct voltage relative to its emitter; two, the drive circuit has some measure of isolation from the power transistors it controls, improving both safety and often noise characteristics.

The design of this transformer is somewhat exacting: to provide fine-grained control and prevent ringing, it should have exceedingly low leakage inductance. Our design process is described in section 5.2.

6

3 Full Bridge & Resonant Load Design

The actual power electronics for this project are deceptively simple.

3.1 Full Bridge

The full bridge is quite standard; its schematic (along with the gate drive schema employed) is given in figure 5. Note the phasing on the drive transformer: for a given input signal, the two transistors on one of the bridge's diagonals will turn on simultaneously, as is necessary for proper operation. In addition to its other advantages, the use of a GDT to drive this bridge prevents "shoot-through," in which both transistors on one side of the bridge turn on at the same time and short the power rails together. There is no possible input signal to the GDT which would cause this to happen.

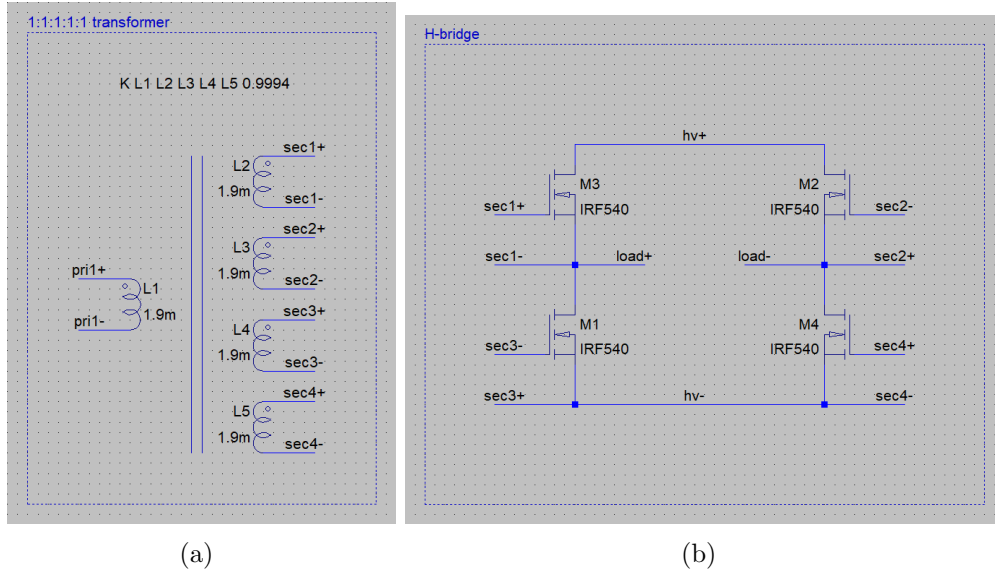(a)   (b)

Figure 5: The gate drive scheme (a), and full-bridge (b).

3.2 Resonant Load

We used a combination series-parallel circuit as our load on the full bridge. The load schematic is given in figure 6. As indicated, the inductor in the

7

parallel LC section is used as the work coil. This load design was inspired by [4] and [5].
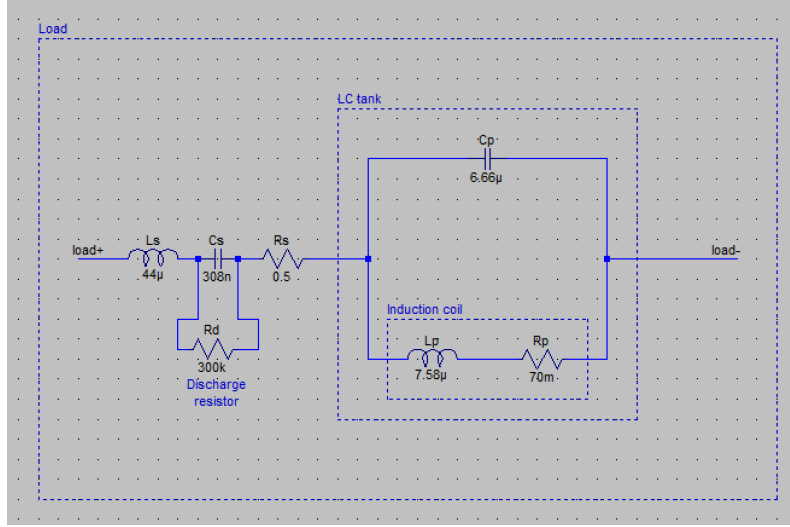

Figure 6: The resonant load used for the bridge.

The load behaves as a bandpass and bandstop filter in series. The oscillator is tuned to the resonant frequency of the parallel LC circuit, which presents its maximum impedance at that frequency. Thus, any current drawn at the fundamental is due to losses in the circuit (hopefully mostly resistive loss in the workpiece). The series LC circuit, tuned to a significantly, higher frequency, serves two purposes: it blocks many of the higher-order harmonics of the drive signal, reducing excess current draw away from the fundamental, and its relatively high resonant frequency helps recirculate reactive currents back into the power rails. Current and voltage waveforms of the load in operation may be found in section 6.1.

Originally, we tuned both LC circuits to the same frequency, which caused two problems: a great deal of the series resonant current never returned to the rails, resulting in a large current draw, and the inductor required for proper operation was prohibitively large. This is a notable case where a terrifically ugly waveform is actually a good goal!

8

4   Simulation Results

Simulation was used extensively in our design process, both to verify results and to prototype new ideas. LTspice was used as our simulation platform, with device-specific models - often created by the device manufacturer when available. In general the simulation outputs agree with our practical results and observations.

Starting in the low voltage section of the circuit, the simulation output matches nicely with our observed results in physical measurements.
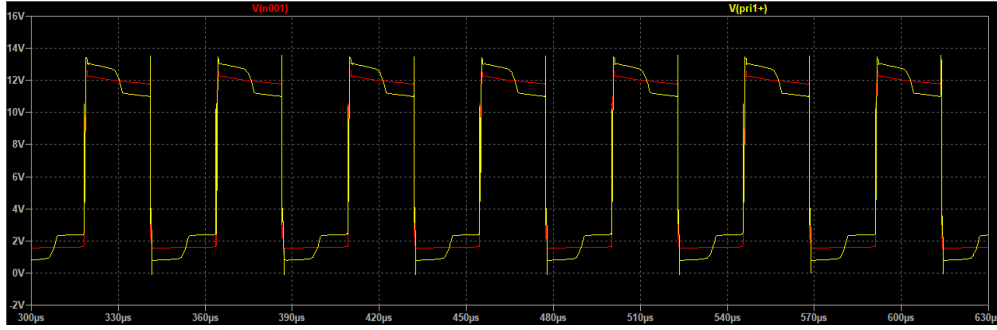

Figure 7: One-sided comparator and buffer voltages.

The LM311's output is represented by the red trace, while the output of the push-pull buffer is seen in yellow, with some distortion caused by it's load - the gate drive transformer. The GDT was also modeled in simulation, along with a simple model of the real component's inductances and coupling characteristics.

$$L_{leak} = L_{wind}(1 - K^2)$$

This expression was used to determine the coupling coefficient K of the gate drive transformer for simulation, where L_{wind} is the inductance of each winding on the transformer, and L_{leak} is the leakage inductance between windings [6]. Leakage inductance was found by measuring the inductance of a winding, with one or more of the other windings shorted together. The coupling coefficient of the transformer was determined to be 0.9994, very nearly ideal.
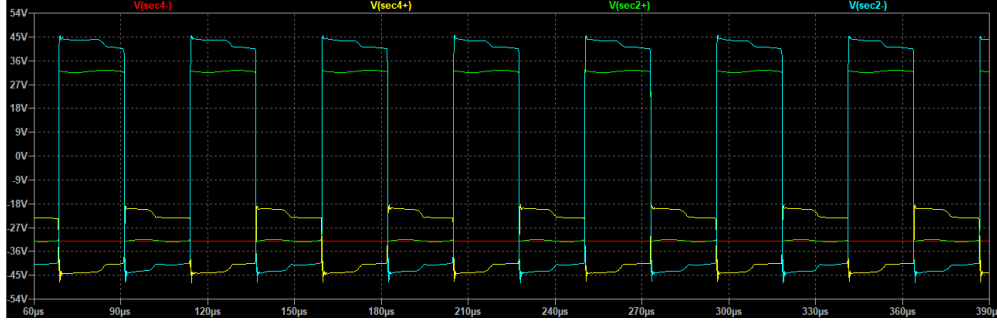
9

Figure 8: Single-sided bridge voltages.

Figure 8 illustrates the various voltage signals surrounding the bridge, and especially, the utility of the GDT. M4's source (red trace) and gate (yellow trace) can be seen switching as desired. M2's source (green trace) can be seen switching the output of the bridge, and it's gate (blue trace) can be seen switching the FET with respect to it's source, all thanks to the GDT.
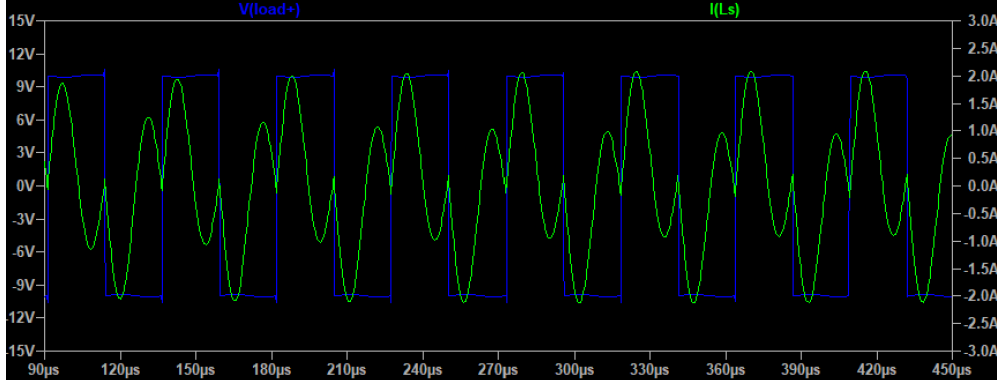

Figure 9: Current through the parallel component of the load.

Figure 9 shows the (nearly) zero-volt switching technique used. The series LC components were tuned to have double the resonant frequency of the parallel LC components, resulting in the current waveform shown here in the green trace.
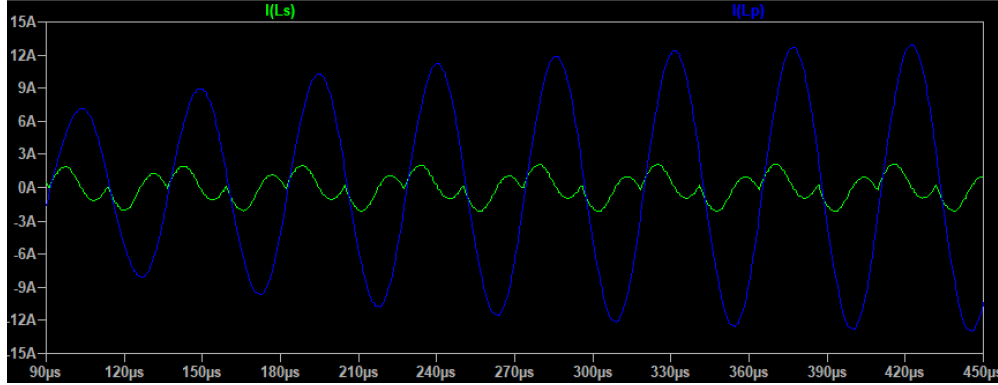
Figure 10: Current through the series and parallel resonant components of the load.

The vastly different peak currents flowing through the series and parallel components of the LC load illustrates the device's ability to maintain a strong alternating magnetic field in the heating area, without pulling an excessive amount of current from the DC supply. These current values were tweaked to match experimental results by adjusting the parallel resistance in the LC tank, since the actual resistance in the tank could not be readily measured. While operating at 10VDC the insertion of the workpiece into the heating coil resulted in a roughly 6A decrease in peak current, which interestingly corresponds to a 36mΩ increase in parallel resistance.

5 Construction

To construct this circuit, we opted to use as many components which were already in the lab as possible, for speed and cost reasons. This led to the choice of IRF540 FETs for the full bridge, the 10 µF resonant capacitors, and the 7555 and LM311s for the control circuitry.

Despite this mindset and the plentiful assortment of components available in the lab, the large-signal nature of our project required us to special-order several parts (described in the following sections).
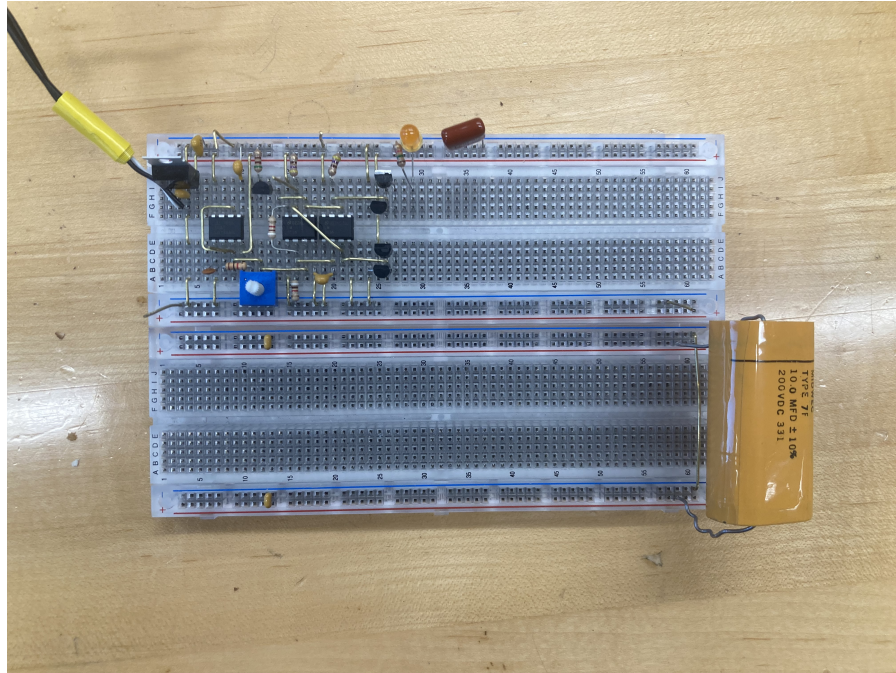
11

5.1 Control Circuitry

Figure 11: The oscillator and gate drive circuitry.

The construction of the control circuitry was straightforward, as all the parts needed were available in the lab. The circuitry used is shown in figure 11. Bare brass wire was used to connect components to save time on stripping and permit more scope probing locations.
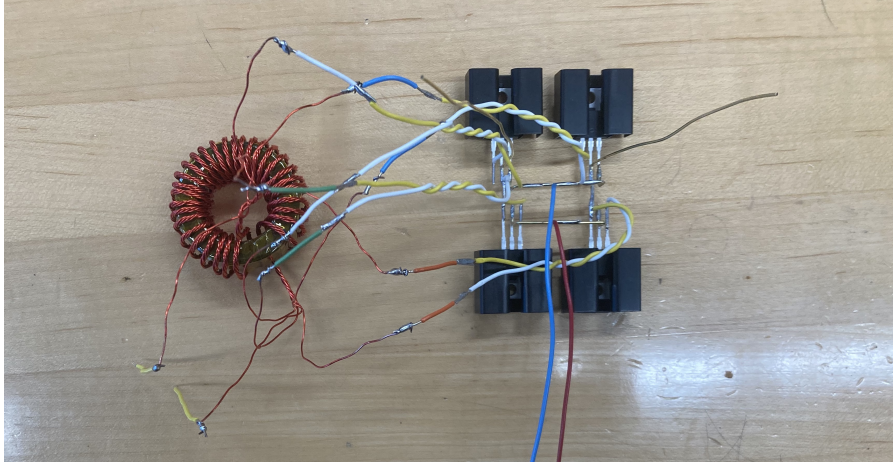
5.2   Gate Drive Transformer & Full Bridge

Figure 12: The gate drive transformer and full bridge.

Due to its stringent design constraints, the gate drive transformer (on the left in figure 12) required special ordering of an appropriate core. The material chosen was #79 from Fair-Rite, as it had low loss and high permeability in our target frequency range. More information may be found in appendix A. The core was insulated with Kapton tape before winding; a previous version of this transformer was wound directly on an uninsulated core, which caused a section of it to incandesce at high bridge voltages due to a short between turns.

The transformer was wound with 30 pentafilar turns of 22 gauge magnet wire. The wire was twisted together with a hand drill prior to winding, to keep the turns close together and thereby reduce the transformer's leakage inductance. The final transformer had an open-circuit inductance of about 2 mH and an input inductance with the output shorted of 2 μH, indicating a coupling coefficient of 0.9994 (well above the minimum acceptable value determined in simulation).

The full bridge (on the right in figure 12) consisted of four IRF540 MOSFETs soldered together in the proper arrangement. We opted to solder the bridge for two reasons: one, the high currents involved were causing unacceptable heating in the breadboard; two, the transistors were growing too warm for open-air operation and needed to be spaced apart to permit the use of heatsinks.

5.3   Series LC Circuit

The series LC circuit had to withstand moderately high currents (on the order of 15 A peak). While not as high as the parallel LC circuit currents, this still presented a design challenge as the required series inductor was several tens of microhenries. Early attempts at series circuits, built with small inductors and one to three film capacitors, were prone to heating (and, on one occasion, explosive destruction). The designs presented in sections 5.3.1 and 5.3.2 are the result of several iterations each.

Correct tuning of the series circuit was accomplished using a fixed series capacitor and a test inductor in the shape of a figure-8. We varied the inductance of this component by varying the distance between the loops of the 8, thus changing the coupled flux between the loops. Once the proper tuning was obtained, the test inductor was measured and a suitable (fixed-value, high-current) replacement was wound.

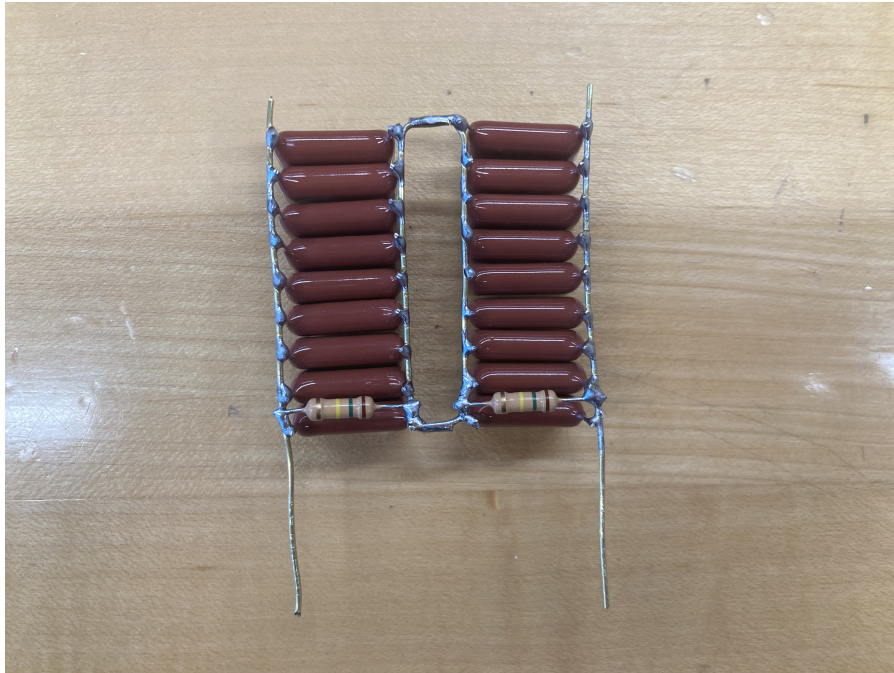### 5.3.1   Series Capacitor

Figure 13: The series capacitor array.

The series capacitor array, shown in figure 13, consists of eighteen 68 nF capacitors in two ranks, yielding an effective capacitance of 0.34 µF. Connecting the capacitors in parallel allowed the array to handle 9 times the maximum current of the individual capacitors in it. Since attempts to use a single film capacitor failed dramatically, this series-parallel array was deemed necessary.

Two 150 kΩ bleeder resistors were wired in parallel with each rank to ensure the capacitors discharge quickly after shutoff. These were added at the behest of Dean Shay after a near Darwin Award at power-off.

5.3.2 Series Inductor

Figure 14: The series inductor.

The series inductor, shown in figure 14, was wound out of lamp cord, as this cord has the required current-carrying capacity. After obtaining the right value for the series inductor (in our case, 36 µH) as described above, we cut a long length of cord and coiled it until the inductor reached the correct value. The ends of the cord were then soldered together or tinned.

The yellow splice visible to the left of the coil is an artifact of the method used to wind it: the coil was wound with bifilar turns at first (as lamp cord contains two conductors), creating two independent coils. These were then electrically connected in series to form a single inductor with twice as many turns.

5.4   Parallel LC Circuit

Figure 15: The parallel LC circuit, consisting of the work coil and the resonant capacitor bank.

The parallel LC circuit, was the part of this project with the most stringent design requirements: to function correctly, it had to have extremely low parasitic resistance (on the order of 70 mΩ!) and be able to handle peak currents in excess of 60 A. Such high currents were necessary due to the atrociously poor coupling through the mug to the workpiece – since magnetic fields around a dipole tend to drop off with the cube of the distance, the necessary spacing of the coil around a mug of tea means that

large magnetic fields must be present in order to couple energy to the workpiece properly.

Despite these challenges, the parallel circuit was relatively easy to build, as it was not very physically complicated. The final work coil and capacitor bank are shown in figure 15.
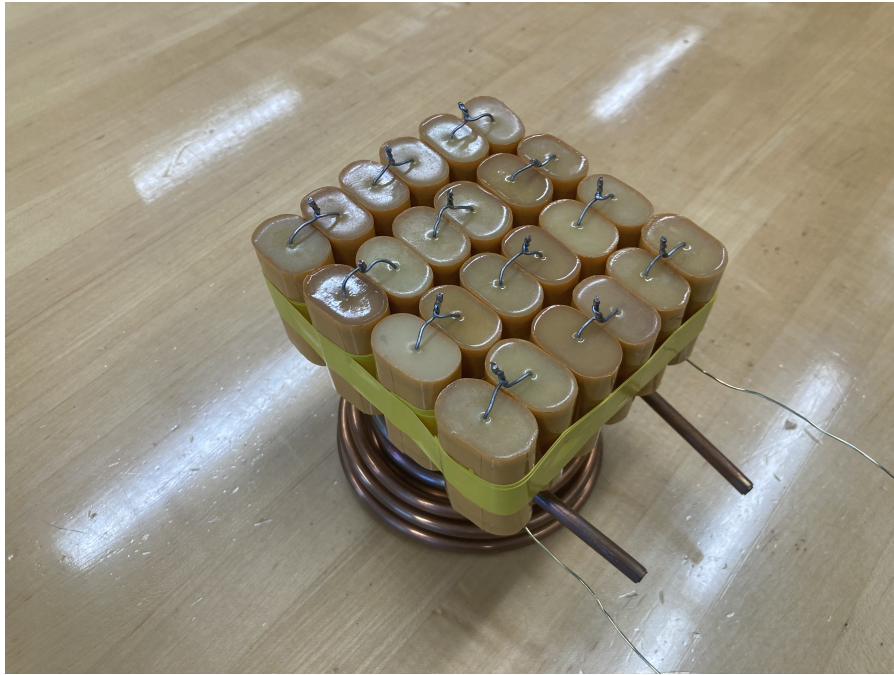
5.4.1 Resonant Capacitor Bank

Figure 16: The bottom side of the parallel LC tank, showing the resonant capacitor bank.

The resonant capacitor bank, shown in figure 16, was constructed out of twenty-four 10 µF film capacitors discovered in a drawer in the lab. These were connected in a series-parallel arrangement for reasons similar to those described in section 5.3.1. The final bank measured approximately 6.7 µF.

5.4.2 Work Coil

We wound the work coil out of half-inch copper tube from McMaster-Carr; more details may be found in appendix A. The coil was wound to

fit snugly around the base of our test mug, so that the iron cube used as the workpiece would be as close to the coil as possible. The coil also supported the mug and prevented its tipping over.

The choice of copper tube for the coil was inspired by the large resonant currents which flowed during heating, and the relatively high frequency of operation. The skin depth of copper at our working frequency of 23 kHz is about 0.4 mm, so use of solid copper wire would be expensive, difficult to bend, and unnecessary.

Note the discoloration of the work coil in figure 15: due to the hot mug sitting on top of it and the high currents flowing through it, the center of the coil still grew extremely hot in testing. This lead to the desoldering of one of the leads, and is considered an open problem with this design.

5.5   Workpiece

In keeping with the "from junk" theme of the project, we used a machined steel cube with several irregular holes in it as the workpiece. This was deemed large enough and ferrous enough to present a theoretically usable load while still being somewhat challenging to work with.

Unfortunately, the cube we found tended to oxidize rather heavily when heated underwater, resulting in a poor environment for brewing tea. In an effort to at least keep the water clearer, we substituted a collection of galvanized washers in later tests.

6   Bench Test Results

6.1   Load Voltage & Current

The testing stage our our project allowed us to refine component values after a preliminary system had been built. Every component had some deviation from its simulation, and so many tweaks were required.

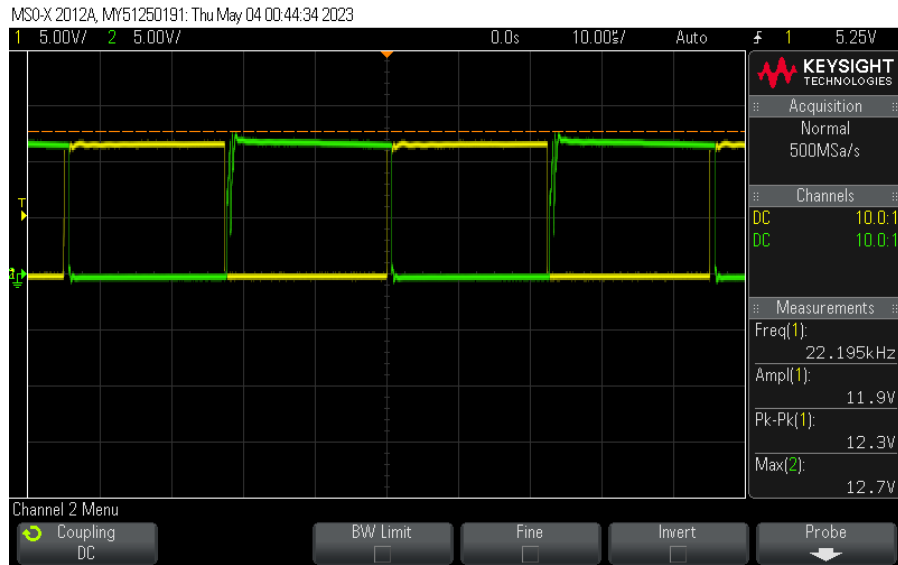As seen below in figure 17, the 7555 timer and comparators worked fine.

Figure 17: The output of the 7555 Timer (green), and smoothed by the comparator (yellow).

The H-bridge operated as expected, though it was large and cumbersome to set up and required active cooling. Not shown here in 18 is the moment the Mk. 1 shorted itself and began to fail.

Figure 18: The differential output of the H-bridge when switching 0V.

Figure 19: The differential output of the H-bridge when switching ~10V.

Building the physical board allowed us to directly tune for the maximum output current by adjusting the frequency of H-bridge signal.
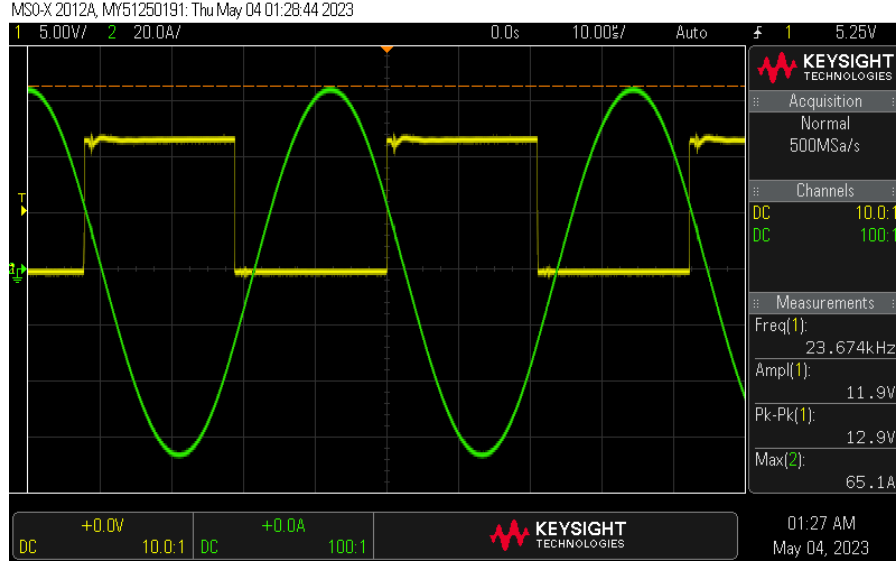

Figure 20: The switched voltage from the H-bridge (yellow), and the induced current flowing between the parallel LC tank (green).

After building the LC tanks, we wanted to see the exact frequency at

which they resonated, to make sure they agreed with our calculations (as seen above in figure 20), and therefore with the frequency of our H-bridge switch. We found the best way to experimentally derive this transfer function was to send a repeating, sinusoidal sweep into the system and plot its output. If we set our window right, it looks like a magnitude response graph, and we can adjust our horizontal spacing to find the exact peak frequency, which was right around 22kHz. Notice the degree of Q.
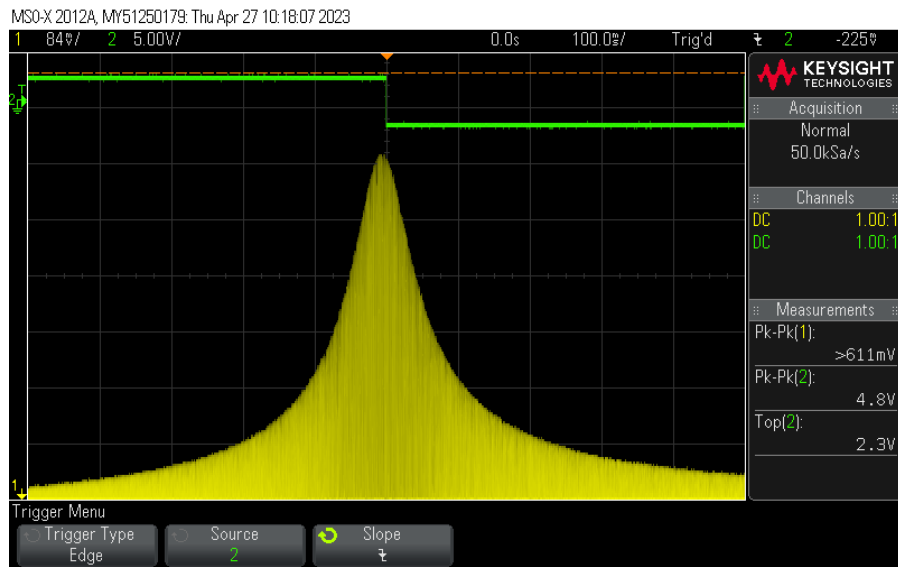

Figure 21: Experimentally-derived resonant frequency of the LC tank.

The series LC tank exhibits a mild band reject and helps filter high frequency noise as mentioned (but real this time). Because the inductor in this LC tank was made from a length of cable looped a number of times, we could tune this LC tank by directly modifying the geometry of the coil. This could include adding or removing turns, adding bends or folds, or separating the turns from each other. This was a second parameter that we could tweak to directly tune the output current.
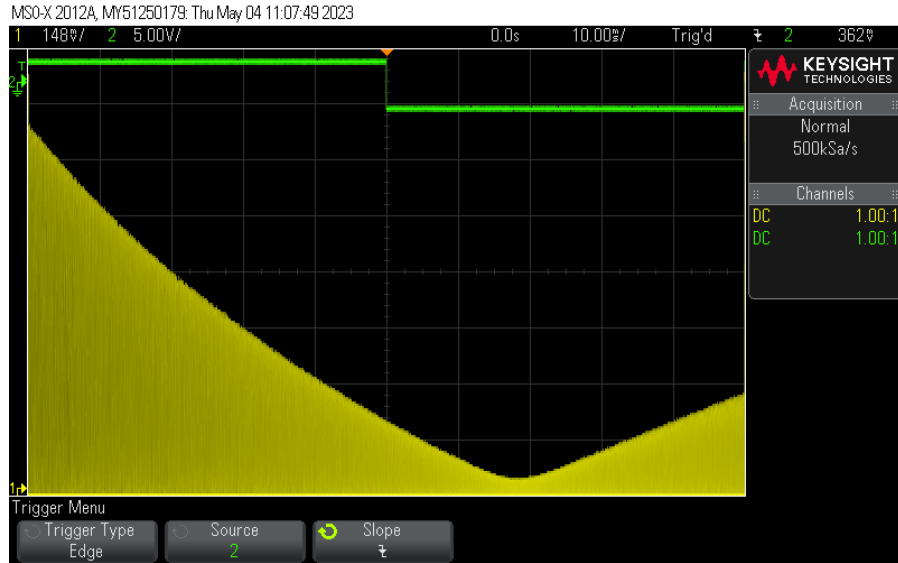
Figure 22: Experimentally derived resonant reject of the series LC circuit.

The signal through the series LC tank has a rather peculiar wave form (seen below in yellow in figure 23), but we assure you that it was chosen and tuned with great care. You will notice that the frequency is double that of the parallel LC tank. This is to keep the power in the series tank from getting too large and drawing too much power, while also keeping the total integral of the wave as close to zero as possible. Secondly, while the h-bridge output isn't plotted below, believe us that the square wave switches right when (yellow) reaches 0V. This keeps the system from wasting energy by making sure most of the power has left the tank before applying power in the other direction.
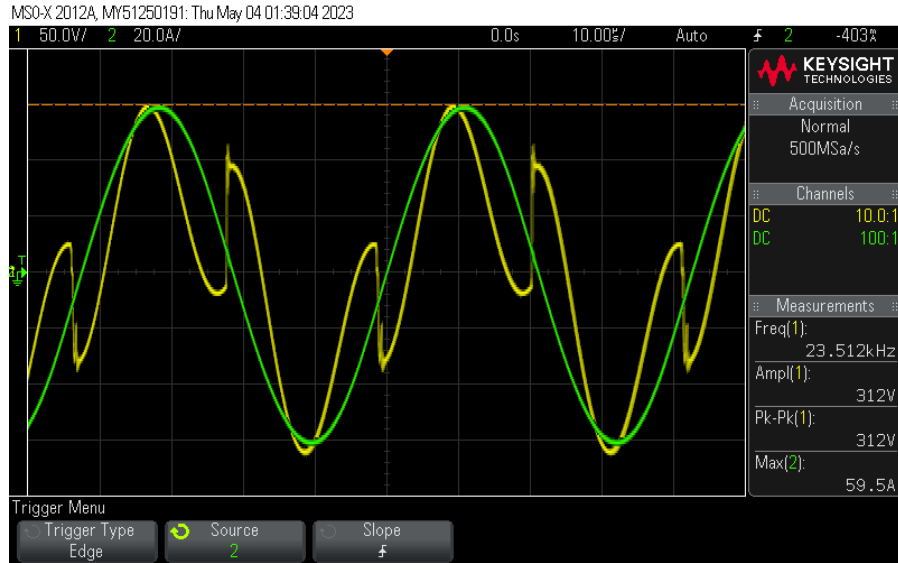
Figure 23: Voltage through the series LC tank (yellow), and current through the parallel LC tank (green).

6.2 Component Stress & Failure

Significant heating of components was observed at all stages of the project, but especially as the tuning improved and the currents in the work coil with it. The series and parallel resonant capacitors were particularly prone to heating, due to the tens of amps flowing through them.

Using the thermal scope we were able to locate hot components (including the tea) and fix the issue before they injured us or worse, failed. For example, our original series LC tank inductor was wrapped with 22 gauge wire, but when it became too hot to touch, we replaced it with a thicker cable. Similarly, the original H-bridge burned itself out before we realized, and the Mk. 2 is now cooled with a fan.

Multiple component failures occurred due to either mis-tuning, over-current, or operator error... but we won't talk about those!

A Components

Name	Price	Link
7555 timer (x1)	$0.95	Digikey
LM311 (x2)	$0.55	Digikey
L7812 (x1)	$0.76	Digikey
IRF540 (x4)	$2.15	Digikey
2N3904 (x3)	$0.12	Digikey
2N3906 (x2)	$0.12	Digikey
#79 toroidial core (x1)	$3.73	Mouser
1/4" copper tubing (10 ft, x1)	$48.15	McMaster-Carr
Total	$63.89	

Table 1: A partial list of components used for this project
.

Table 1 is necessarily incomplete, as some parts used (e.g., the parallel resonant capacitors) were not available from any retailer we could find. Other parts which were still available but common (resistors, ceramic capacitors, etc.) were omitted, as they are not expensive and any electronics shop would already have them on hand.

References

[1] V. Rudnev, D. Loveless, and R. L. Cook, *Handbook of Induction Heating*. CRC Press, 2nd ed., 2017.

[2] S. Wang, K. Izaki, I. Hirota, H. Yamashita, H. Omori, and M. Nakaoka, "Induction-Heated Cooking Appliance Using New Quasi-Resonant ZVS-PWM Inverter With Power Factor Correction," *IEEE Transactions on Industry Applications*, vol. 34, July/August 1998.

[3] W. Han, K. T. Chau, C. Jiang, and W. Liu, "All-Metal Domestic Induction Heating Using Single-Frequency Double-Layer Coils," *IEEE Transactions on Magnetics*, vol. 54, November 2018.

[4] Hackaday, "Keep Coffee Warm Through Induction Heating."

[5] S. Ward, "CCPS Design."

[6] M. Engelhardt, "Using Transformers in LTspice/Switcher CAD III," tech. rep.